

# Relating frontier orbital energies from voltammetry and photoelectron spectroscopy to the open-circuit voltage of organic solar cells

**Citation for published version (APA):**

Willems, R. E. M., Weijtens, C. H. L., de Vries, X., Coehoorn, R., & Janssen, R. A. J. (2019). Relating frontier orbital energies from voltammetry and photoelectron spectroscopy to the open-circuit voltage of organic solar cells. *Advanced Energy Materials*, 9(10), [1803677]. <https://doi.org/10.1002/aenm.201803677>

**DOI:**

[10.1002/aenm.201803677](https://doi.org/10.1002/aenm.201803677)

**Document status and date:**

Published: 13/03/2019

**Document Version:**

Publisher's PDF, also known as Version of Record (includes final page, issue and volume numbers)

**Please check the document version of this publication:**

- A submitted manuscript is the version of the article upon submission and before peer-review. There can be important differences between the submitted version and the official published version of record. People interested in the research are advised to contact the author for the final version of the publication, or visit the DOI to the publisher's website.
- The final author version and the galley proof are versions of the publication after peer review.
- The final published version features the final layout of the paper including the volume, issue and page numbers.

[Link to publication](#)

**General rights**

Copyright and moral rights for the publications made accessible in the public portal are retained by the authors and/or other copyright owners and it is a condition of accessing publications that users recognise and abide by the legal requirements associated with these rights.

- Users may download and print one copy of any publication from the public portal for the purpose of private study or research.
- You may not further distribute the material or use it for any profit-making activity or commercial gain
- You may freely distribute the URL identifying the publication in the public portal.

If the publication is distributed under the terms of Article 25fa of the Dutch Copyright Act, indicated by the "Taverne" license above, please follow below link for the End User Agreement:

[www.tue.nl/taverne](http://www.tue.nl/taverne)

**Take down policy**

If you believe that this document breaches copyright please contact us at:

[openaccess@tue.nl](mailto:openaccess@tue.nl)

providing details and we will investigate your claim.

# Relating Frontier Orbital Energies from Voltammetry and Photoelectron Spectroscopy to the Open-Circuit Voltage of Organic Solar Cells

Robin E. M. Willems, Christ H. L. Weijtens, Xander de Vries, Reinder Coehoorn, and René A. J. Janssen\*

For 19 diketopyrrolopyrrole polymers, the highest occupied molecular orbital (HOMO) energies are determined from i) the oxidation potential with square-wave voltammetry (SWV), ii) the ionization potential using ultraviolet photoelectron spectroscopy (UPS), and iii) density functional theory (DFT) calculations. The SWV HOMO energies show an excellent linear correlation with the open-circuit voltage ( $V_{oc}$ ) of optimized solar cells in which the polymers form blends with a fullerene acceptor ([6,6]-phenyl- $C_{61}$ -butyl acid methyl ester or [6,6]-phenyl- $C_{71}$ -butyl acid methyl ester). Remarkably, the slope of the best linear fit is  $0.75 \pm 0.04$ , i.e., significantly less than unity. A weaker correlation with  $V_{oc}$  is found for the HOMO energies obtained from UPS and DFT. Within the experimental error, the SWV and UPS data are correlated with a slope close to unity. The results show that electrochemically determined oxidation potentials provide an excellent method for predicting the  $V_{oc}$  of bulk heterojunction solar cells, with absolute deviations less than 0.1 V.

(CT) state ( $E_{CT}$ ) plays a crucial role in determining  $V_{oc}$ .<sup>[1]</sup> When free carrier generation occurs via dissociation of relaxed CT states, the relation between  $E_{CT}$  and  $V_{oc}$  in the notation proposed by Vandewal is<sup>[1]</sup>

$$qV_{oc} = E_{CT} - kT \ln \left( \frac{(k_r + k_{nr}) N_{CTC}}{G} \right) \quad (1)$$

where  $q$  is the electron charge,  $k$  is the Boltzmann constant,  $T$  is the temperature,  $k_r$  and  $k_{nr}$  are the radiative and nonradiative decay constants of the CT state, respectively,  $N_{CTC}$  is the total volume density of CT complexes, and  $G$  is the generation rate of electron-hole pairs, which is proportional to flux of absorbed photons. Note that Equation (1) is similar to relations where an effective band gap ( $E_g^{eff}$ ) was used instead of  $E_{CT}$ , defined as the difference between the electron affinity

## 1. Introduction


In organic bulk heterojunction solar cells, the open-circuit voltage ( $V_{oc}$ ) depends on the properties of donor and acceptor materials, the blend morphology, and the experimental conditions such as the light intensity and temperature. In recent years, it has become clear that the energy of the interfacial charge-transfer

of the acceptor and the ionization potential of the donor.<sup>[2–4]</sup> In agreement with Equation (1), temperature- and light intensity-dependent measurements have shown that the extrapolated values of  $E_{CT}$  and  $V_{oc}$  become equal in the  $T = 0$  K limit.<sup>[5–7]</sup> The second term on the right-hand side of Equation (1) has initially been found to be approximately constant ( $\approx 0.6$  eV) for many different donor and acceptor blends when the corresponding cells are measured under AM1.5G (100 mW cm<sup>-2</sup>) conditions at room temperature, such that  $qV_{oc} \propto E_{CT}$ .<sup>[1]</sup> Considering that, for efficient charge generation, the optical band gap of the blend ( $E_g$ ) should be equal to or larger than  $E_{CT}$ , this result is in accordance with the experimental observation that for present organic solar cells the minimum photon energy loss ( $E_g - qV_{oc}$ ) is about 0.6 eV.<sup>[8,9]</sup> A recent more detailed study covering a broader range, however, provides evidence that the magnitude of the second term on the right-hand side of Equation (1) slightly decreases when  $E_{CT}$  increases, resulting in an overall slope of  $qV_{oc}$  versus  $E_{CT}$  that is somewhat larger than unity ( $qV_{oc} \propto 1.08 \times E_{CT}$ ).<sup>[10]</sup> Because the nonradiative voltage loss is high compared to other photovoltaic technologies, the development of new organic semiconductors for solar cells is currently focused on decreasing the voltage losses incurred in converting solar light.

The energy of the CT state can experimentally be determined from the optical absorption or emission spectra of blends,

R. E. M. Willems, Dr. C. H. L. Weijtens, X. de Vries, Prof. R. Coehoorn, Prof. R. A. J. Janssen  
Molecular Materials and Nanosystems & Institute for Complex Molecular Systems  
Eindhoven University of Technology  
P.O. Box 513, 5600 MB Eindhoven, The Netherlands  
E-mail: r.a.j.janssen@tue.nl

Prof. R. A. J. Janssen  
Dutch Institute for Fundamental Energy Research  
De Zaale 20, 5612 AJ Eindhoven, The Netherlands

 The ORCID identification number(s) for the author(s) of this article can be found under <https://doi.org/10.1002/aenm.201803677>.

© 2019 The Authors. Published by WILEY-VCH Verlag GmbH & Co. KGaA, Weinheim. This is an open access article under the terms of the Creative Commons Attribution-NonCommercial License, which permits use, distribution and reproduction in any medium, provided the original work is properly cited and is not used for commercial purposes.

DOI: 10.1002/aenm.201803677

which are fundamentally related to each other.<sup>[1,11,12]</sup> Most commonly, it is measured from fitting the low-energy tail of the external quantum efficiency spectrum of the solar cell.<sup>[1]</sup> This has the drawback that for the most interesting donor–acceptor combinations, the CT absorption will be hidden under the  $S_0 \rightarrow S_1$  optical absorption of the donor or acceptor absorption, because in efficient solar cells the loss from  $S_1$  state to CT state would be minimized. Other methods used to determine  $E_{CT}$  are ultraviolet photoemission spectroscopy and charge-modulated electroabsorption spectroscopy.<sup>[13]</sup> For designing new materials and photoactive blends, it is important to be able to predict and understand  $V_{oc}$  from the properties of the donor and acceptor alone.  $E_{CT}$  is related to the energy difference of the highest occupied molecular orbital (HOMO) of the electron donor ( $E_{HOMO,D}$ ) and the lowest unoccupied molecular orbital (LUMO) of the electron acceptor ( $E_{LUMO,A}$ ) used in the bulk heterojunction blend.<sup>[14]</sup> For mixed stack organic charge-transfer solids composed of planar aromatic donor and acceptor molecules,  $E_{CT}$  has been found to be proportional to the difference between the redox potentials determined by electrochemical methods and was expressed as  $E_{CT} = |E_{HOMO,D} - E_{LUMO,A}| - \Delta$ ,<sup>[15]</sup> in which  $\Delta$  is the attractive ion–ion Coulomb interaction between the ion pair. For organic CT complexes in solid and solution, a similar linear dependence has been found with the redox energy levels, however, with slopes that are in the range from 0.82 to 0.94, i.e., generally slightly less than unity, and sometimes also dependent on the specific class of materials.<sup>[16–18]</sup> The empirical relation  $qV_{oc} = |E_{HOMO,D} - E_{LUMO,A}| - 0.3$  eV has been the basis of much of the OPV material design.<sup>[19–21]</sup> This relation implies that  $V_{oc}$  increases linearly, with a slope of 1, when  $E_{HOMO,D}$  becomes more negative. On the other hand, the donor and acceptor molecular orbitals may interact at their interface, resulting in hybridized energy levels.<sup>[22]</sup> Similarly, a vacuum level shift may occur at the donor–acceptor interface as a result of an interface dipole.<sup>[7]</sup> In both latter cases, the energy difference  $|E_{HOMO,D} - E_{LUMO,A}|$  increases and  $V_{oc}$  would no longer increase with slope 1 with a decreasing  $E_{HOMO,D}$ . Predicting the energy level alignment at donor–acceptor interfaces from the ionization energy and electron affinity of the organic materials forming the heterojunction has been found challenging<sup>[23]</sup>; hence, it is a priori not clear which slope to expect.

In addition, there is an almost permanent discussion on which technique is most suitable for determining the  $E_{HOMO,D}$  and  $E_{LUMO,A}$  energies accurately. Ultraviolet photoelectron spectroscopy (UPS),<sup>[24]</sup> (low-energy) inverse photoemission spectroscopy,<sup>[25,26]</sup> photoelectron yield spectroscopy also known as photoelectron spectroscopy in air,<sup>[27–29]</sup> and cyclic voltammetry (CV) are the main techniques used to determine ionization potentials and electron affinities. Each of these techniques, however, is susceptible to experimental difficulties. In UPS, there is a difference in the ionization energy between molecules at the surface and in the bulk.<sup>[30]</sup> For CV, determining peak positions of redox waves can be compromised by the fact that the redox processes may lack electrochemical or even chemical reversibility, which influences the shape of the curve. An alternative to CV is square-wave voltammetry (SWV).<sup>[31,32]</sup> Compared to CV, SWV has several experimental advantages. In SWV, a square-wave potential is applied on top of a stepwise-ramped potential and the current is measured in each step

during the application of both the forward and backward potential waves. As the charging current decays with time ( $t$ ) as  $e^{-t/RC}$ , with  $RC$  the effective resistance ( $R$ ) and capacitance ( $C$ ) product of the system, and the Faradaic current with  $t^{-1/2}$ , the charging current in square-wave voltammetry experiments is usually negligible.<sup>[31,33]</sup> By plotting the current difference at each potential step, only reversible processes are taken into account. The molecular orbital energy ( $E_{MO,CV}$ ) relative to the vacuum level energy can be determined from CV or SWV measurements via  $E_{MO,CV} = -(qE_{CV}^{onset} + E_{Fc/Fc^+})$  with  $E_{Fc/Fc^+}$  the ionization energy of the ferrocene/ferrocenium ( $Fc/Fc^+$ ) redox couple.  $Fc/Fc^+$  is one of the redox couples recommended by the International Union of Pure and Applied Chemistry for reporting energy levels in nonaqueous solvents.<sup>[34]</sup> In the literature, there is little consensus about the correct vacuum energy level of the  $Fc/Fc^+$  redox couple, as values between  $-4.4$  and  $-5.4$  eV have been reported and used.<sup>[35]</sup>

Recently, several experimental studies of the oxidation potential as obtained from CV ( $E_{ox,CV}$ ) and ionization potential from UPS (IP) have revealed that both quantities are linearly correlated, i.e.,  $IP = \alpha^+ qE_{ox,CV} + \beta^+$ , but that the best-fit slope varies considerably from  $\alpha^+ = 0.9$  to 1.5, depending on the material class.<sup>[36–40]</sup> This would alter the proportionality constant between  $E_{CT}$  and  $(E_{HOMO,D} - E_{LUMO,A})$ . Most of these comparative studies, however, did not address the question which technique yields the most accurate data to correlate with the  $V_{oc}$  for organic solar cells. Only in a recent paper by Fahlman and coworkers, it was argued that the precision of the CV-derived ionization potentials is not sufficient.<sup>[40]</sup> It is therefore at present not clear which experimental technique for determining  $(E_{HOMO,D} - E_{LUMO,A})$  is most suitable for accurately predicting  $V_{oc}$ .

Here we determine the HOMO energies of 19 different diketopyrrolopyrrole (DPP)-based polymers, previously synthesized by our group (Figure 1),<sup>[41]</sup> using CV, SWV, UPS, and density functional theory (DFT) calculations and correlate these with the  $V_{oc}$  of the corresponding solar cells in which the polymer is used as donor in combination with [6,6]-phenyl-C<sub>61</sub>-butyl acid methyl ester (PC<sub>61</sub>BM) or [6,6]-phenyl-C<sub>71</sub>-butyl acid methyl ester (PC<sub>71</sub>BM) as acceptor. DPP polymer–fullerene solar cells can reach power conversion efficiencies over 9%.<sup>[42–44]</sup> These polymers consist of an electron-deficient DPP unit that alternates along the chain with an electron-rich  $\pi$ -conjugated segment, creating a donor–acceptor-type polymer. The optical band gap has been tuned from 1.13 to 1.73 eV by changing the  $\pi$ -conjugated segment. By employing appropriate synthetic procedures, we are confident that adverse homocoupling reactions that can strongly effect the energy levels in these alternating copolymers are virtually absent in the materials studied.<sup>[45]</sup> All experiments have been performed on layers applied via the same technique and under controlled circumstances, to maximize comparability of the data. This also holds for the morphology of the photovoltaic layers, which consists in each case of an intimately mixed blend with nanometer-wide semicrystalline polymer fibrils.<sup>[41]</sup> We investigate which technique can provide the most accurate prediction for the  $V_{oc}$  of an optimized solar cell as determined under simulated standard solar illumination (AM1.5G spectrum at 100 mW cm<sup>-2</sup>). We find that, within experimental error, the SWV and UPS data are correlated with a slope close to unity,

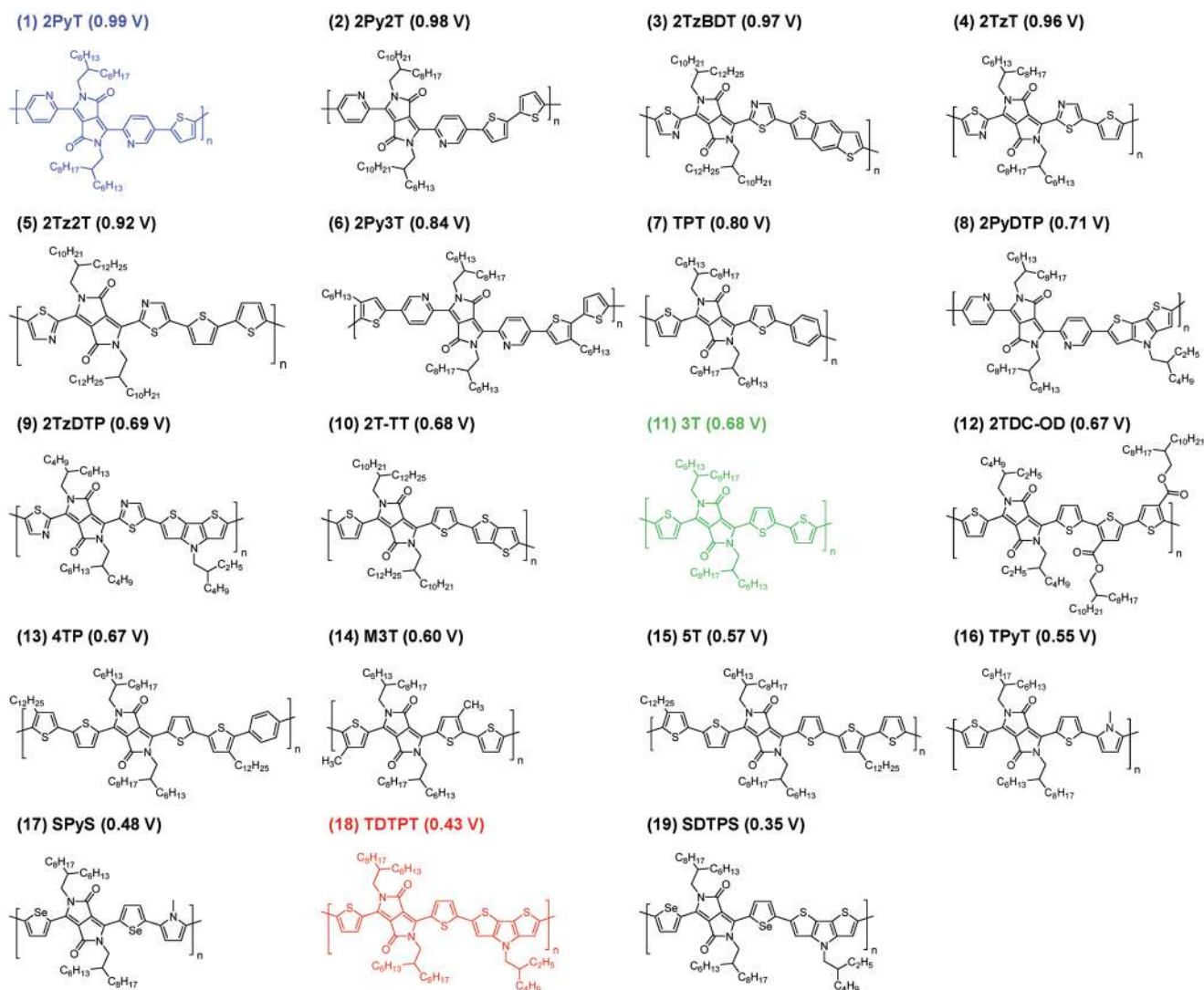


**Figure 1.** Structures of the DPP-based polymers displayed in order of decreasing  $V_{oc}$  (indicated in parentheses) as measured in bulk heterojunction solar cells with PC<sub>61</sub>BM or PC<sub>71</sub>BM as acceptor. For brevity, the leading part of the polymer name (PDPP) has been omitted. The color coding indicated (blue, green, and red for three exemplary materials with a large, intermediate, and small  $V_{oc}$ , respectively) has been used throughout the paper. Details on solar cell architectures, photovoltaic parameters, and literature references can be found in the Supporting Information.

and that  $V_{oc}$  is most strongly correlated with the oxidation potential as obtained from SWV, but with a slope significantly less than unity. Possible reasons for this remarkable result are discussed.

## 2. Results and Discussion

### 2.1. Cyclic and Square-Wave Voltammetry

Cyclic and square-wave voltammetry experiments were performed for all DPP polymers shown in Figure 1 as thin films on a platinum wire, immersed in acetonitrile containing tetrabutylammonium hexafluorophosphate as electrolyte. As an example, **Figure 2** shows the CV and SWV oxidation waves of 2PyT (1), 3T (11), and TDTP (18), for which the  $V_{oc}$  in bulk heterojunction solar cells with PCBM as the common

acceptor varies over a considerable range, i.e., from 0.43 to 0.99 V (Figure 1 and **Table 1**). The cyclic and square-wave voltammograms of all polymers are collected in the Supporting Information. Figure 2 shows that not in all cases clear peaks are observed in both CV and SWV. For example, the SWV of 3T only shows a broad maximum, for which it is impossible to determine a well-defined peak position. Taking the onset, which can be determined as the intercept of the tangent in the inflection point with the baseline, is a more consistent method. For most polymers, the onset potentials of CV and SWV determined in this way differ only by up to  $\pm 0.05$  V, but in some cases capacitive contributions to the redox currents cause an apparent shift in the onset potential. Figure 2 shows that this shift is especially distinct for 2PyT. SWV eliminates this artifact, and for these reasons, we focus in the remainder on the onset potentials as obtained from SWV. We estimate the accuracy to be  $\pm 0.05$  V. We note that in previous publications that reported

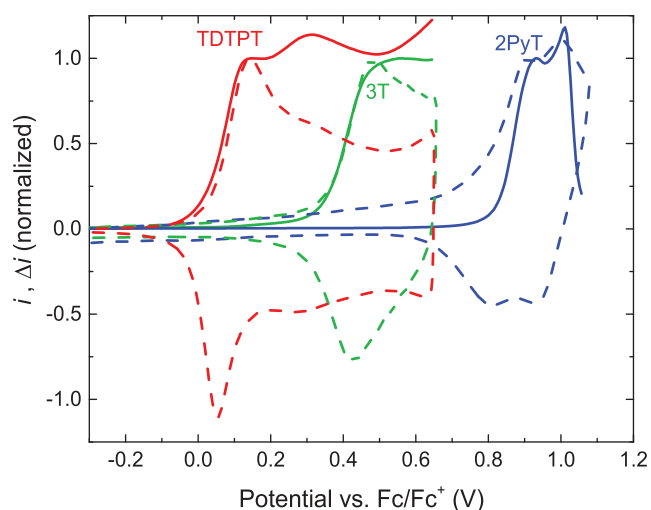


**Figure 2.** Square-wave voltammograms ( $\Delta i$ , solid lines) and cyclic voltammograms ( $i$ , dashed lines) for three selected polymers: 2PyT (**1**), 3T (**11**), and TDTPT (**18**). The oxidation potential ( $E_{\text{ox,SWV}}$ , Table 1) is determined by the intercept of the tangent through the inflection point at the edge of the square-wave voltammogram and the baseline.

the synthesis and photovoltaic properties of the DPP polymers discussed here (see References in the Supporting Information for details), CV measurements have been performed on the DPP-based polymers in solution or on thin films on indium tin oxide (ITO) substrates. Our present results from SWV, for thin films on a platinum wire, reproduce the oxidation potential reported previously in all cases where the reported oxidation

potential was measured on thin films (Figure S1, Supporting Information) within the measurement uncertainty ( $\pm 0.05$  V). However, the oxidation potential of polymers measured when dissolved in the electrolyte solution can differ up to 0.5 V. These differences can, at least in part, be attributed to the fact that interactions between polymer chains in a solid film affect the energy levels compared to molecularly dissolved chains in solution, similar to the well-known changes in optical band gap when going from solution to film.<sup>[46]</sup>

The SWV redox potentials ( $E_{\text{ox,SWV}}$  and  $E_{\text{red,SWV}}$ ) of all polymers are listed in Table 1. The polymers with electron-deficient aromatic units flanking the DPP unit such as pyridine-2,6-diyl or thiazoyl-2,5-diyl groups have the highest oxidation potentials, while those with electron-rich selenophene-2,5-diyl or dithieno[3,2-*b*:2',3'-*d*]pyrrole-2,6-diyl units have the lowest oxidation potentials. As a result of the different combinations of heterocycles used in the  $\pi$ -conjugated segments, the oxidation potentials cover a relatively broad range from  $-0.05$  to  $0.82$  V versus  $\text{Fc}/\text{Fc}^+$ . **Figure 3** shows that the oxidation potentials of the DPP polymers ( $E_{\text{ox,SWV}}$ ) and the  $V_{\text{oc}}$  of optimized solar cells (measured under AM1.5G ( $100 \text{ mW cm}^{-2}$ ) illumination) in blends with  $\text{PC}_{61}\text{BM}$  or  $\text{PC}_{71}\text{BM}$  are strongly correlated. A linear fit yields

$$V_{\text{oc}} = (0.75 \pm 0.04)E_{\text{ox,SWV}} + (0.40 \pm 0.02) [\text{V}] \quad (2)$$

The  $R$ -square value is  $R^2 = 0.94$ . It is noteworthy that the slope that emerges from the fit is less than unity. An alternative way of fitting is the Deming regression,<sup>[47]</sup> which is a technique for fitting a straight line to 2D data where both

**Table 1.** SWV redox potentials and HOMO energies from UPS and DFT for DPP polymers.

Polymer	$V_{\text{oc}}^{\text{a)}$ [V]	$E_{\text{ox,SWV}}^{\text{b)}$ [V]	$E_{\text{red,SWV}}^{\text{b)}$ [V]	$E_{\text{g,SWV}}$ [eV]	$E_{\text{g,opt}}^{\text{a)}$ [eV]	$E_{\text{HOMO,SWV}}^{\text{c)}$ [eV]	$E_{\text{HOMO,UPS}}$ [eV]	$E_{\text{HOMO},\Delta\text{SCF}}$ [eV]	
1	2PyT	0.99	0.82	-1.38	2.20	1.73	-5.41	-5.50	-5.87
2	2Py2T	0.98	0.71	-1.43	2.14	1.70	-5.31	-5.06	-5.72
3	2TzBDT	0.97	0.75	-1.24	1.99	1.53	-5.34	-5.29	-5.67
4	2TzT	0.96	0.75	-1.25	2.00	1.44	-5.34	-5.27	-5.84
5	2Tz2T	0.92	0.68	-1.31	1.99	1.47	-5.27	-5.22	-5.73
6	2Py3T	0.84	0.51	-1.48	1.99	1.68	-5.10	-5.06	-5.51
7	TPT	0.80	0.45	-1.54	1.99	1.53	-5.04	-4.94	-5.54
8	2PyDTP	0.71	0.27	-1.43	1.70	1.54	-4.86	-4.88	-5.52
9	2TzDTP	0.69	0.40	-1.32	1.72	1.28	-4.99	-5.30	-5.47
10	2T-TT	0.68	0.37	-1.52	1.89	1.35	-4.96	-4.85	-5.45
11	3T	0.68	0.34	-1.46	1.80	1.30	-4.93	-4.87	-5.49
12	2TDC-OD	0.67	0.51	-1.42	1.93	1.39	-5.10	-4.92	-5.43
13	4TP	0.67	0.40	-1.61	2.01	1.54	-4.99	-4.90	-5.38
14	M3T	0.60	0.24	-1.50	1.74	1.30	-4.83	-5.01	-5.40
15	5T	0.57	0.27	-1.53	1.80	1.45	-4.86	-4.61	-5.22
16	TPyT	0.55	0.23	-1.63	1.86	1.34	-4.82	-4.82	-5.38
17	SPyS	0.48	0.14	-1.57	1.71	1.24	-4.73	-4.71	-5.36
18	TDTPT	0.43	0.02	-1.56	1.58	1.23	-4.61	-4.48	-5.18
19	SDTPS	0.35	-0.05	-1.51	1.46	1.13	-4.54	-4.64	-5.16

<sup>a)</sup> $E_{\text{g,opt}}$  and  $V_{\text{oc}}$  were obtained from the literature; see the Supporting Information for details; <sup>b)</sup>Versus  $\text{Fc}/\text{Fc}^+$ ; <sup>c)</sup>Determined from  $E_{\text{ox,SWV}}$  using  $E_{\text{Fc}/\text{Fc}^+} = -4.59$  eV.

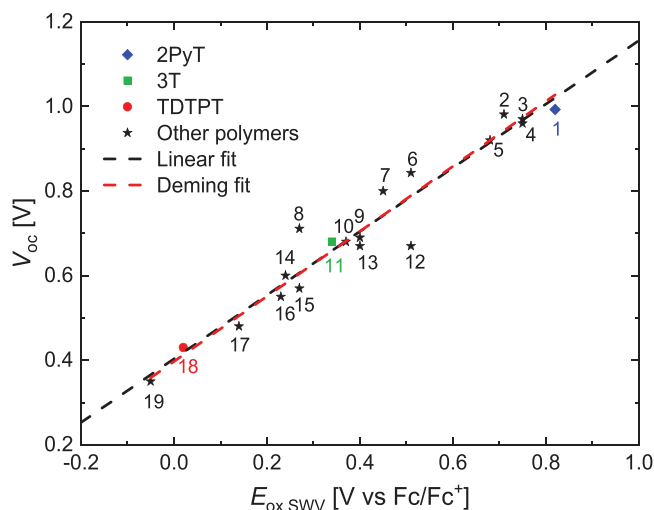


**Figure 3.** Open-circuit voltage ( $V_{oc}$ ) of DPP polymer:PCBM solar cells versus SWV oxidation potentials ( $E_{ox,SWV}$ ) of DPP polymers. The labels indicate the polymers in Figure 1. The black dashed line is a linear regression fit, given by Equation (2) (slope 0.75,  $R^2 = 0.94$ ). The red dashed line represents a Deming regression with slope = 0.77 and  $R^2 = 0.94$ .

variables are measured with error. The Deming regression gives virtually identical results ( $V_{oc} = 0.77E_{ox,SWV} + 0.40$  V,  $R^2 = 0.94$ ) and is shown as the red dashed line in Figure 3.

Whereas the oxidation potentials vary substantially across the set of DPP polymers studied over a 0.87 V wide range, the range of variation of the reduction potentials, 0.39 V, is relatively small. Hence, the conjugated segments between the DPP groups have smaller effect on the LUMO energy than on the HOMO energy. Nevertheless, a clear correlation is present with the electronic nature of the aromatic units flanking the DPP unit. Polymers with flanking thiazoyl-2,5-diyls have  $-1.24$  V  $\geq E_{red,SWV} \geq -1.32$  V, those with pyridine-2,6-diyls have  $-1.38$  V  $\geq E_{red,SWV} \geq -1.43$  V, while those with thiophene-2,5-diyls or selenophene-2,5-diyls have  $-1.42$  V  $\geq E_{red,SWV} \geq -1.61$  V. These rather distinct ranges demonstrate that the LUMO extends from the DPP core into the flanking aromatic unit, but to a lesser extent into the remainder of the conjugated segment.

For the DPP polymers, the electrochemical band gap, defined as  $E_{g,SWV} \equiv q(E_{ox,SWV} - E_{red,SWV})$ , is larger than the optical band gap ( $E_{g,opt}$ ) determined from the onset of absorption in thin films (Table 1). **Figure 4** reveals that the electrochemical gap and optical gap are strongly correlated. The dashed line in Figure 4 represents a fit with a fixed slope of unity to the data  $E_{g,opt} = E_{g,SWV} - (0.44 \pm 0.02)$  [eV]. For most DPP polymers, the optical and electrochemical band gaps adhere to this relation ( $R^2 = 0.72$ ), but exceptions are evident, especially for 2PyDTP (8) and to lesser extent for 2Py3T (6), 5T (15), TDTPT (18), and SDTPS (19). If we view  $E_{g,SWV}$  as the single-particle gap (sometimes called the transport gap), the dashed line in Figure 4 indicates that the effective singlet exciton binding energy is  $\approx 0.44$  eV, quite independent of the specific polymer (apart from the exceptions noted). The average effective binding energy, determined empirically as  $E_b = E_{g,SWV} - E_{g,opt}$ , amounts to 0.44 eV and reflects a combination of fundamental effects (such as Coulomb and exchange interactions) and experimental

effects (such as the presence of electrolyte ions in the oxidized or reduced films that may affect the absolute and relative values of the redox potentials). We also note that the actual  $E_b$  value will depend on how the optical and electrochemical gaps are determined. We used the onsets of the absorbance spectrum and the square-wave voltammogram as determined by the crossing of tangent in the inflection point and the baseline. Hence, the value should be treated with caution. The value of the singlet exciton binding energy in semiconducting polymers has been subject to intense discussions, as it has been notoriously difficult to agree on the method how it can be determined experimentally. Many-body theoretical calculations of the excitonic properties of conjugated polymers that include the interchain screening of the Coulomb interaction by using the bulk dielectric constant have revealed binding energies of 0.4–0.6 eV for a number of homopolymers,<sup>[48]</sup> consistent with the present result for donor–acceptor DPP polymers. For small-molecule organic semiconductors, the singlet exciton binding energy is often much larger.<sup>[37,49–51]</sup>

It is of interest to consider why polymers 2PyDTP (8), 2Py3T (6), 5T (15), TDTPT (18), and SDTPS (19) differ from the other DPP polymers. For 2PyDTP (8), the effective binding energy is as low as  $E_b = 0.16$  eV, while for the other four it falls in the range  $0.31 \leq E_b \leq 0.36$ , still less than the 0.44 eV difference represented by the dashed line in Figure 4. Out of the entire series of DPP polymers, 2PyDTP comprises the most distinct combination of an electron-rich unit (DTP, 4*H*-dithieno[3,2-*b*:2',3'-*d*]pyrrole) and an electron-deficient unit (2Py-DPP-2Py, 3,6-di(pyridin-2-yl)-2,5-dihydropyrrolo[3,4-*c*]pyrrole-1,4-dione). In such case, it can be expected that the lowest excited singlet state has a more pronounced charge-transfer character, in which the positive and negative charge densities are more localized on different units than for the other materials. Because of the localization, the singlet exciton binding energy is reduced. The same, but to a lesser extent,

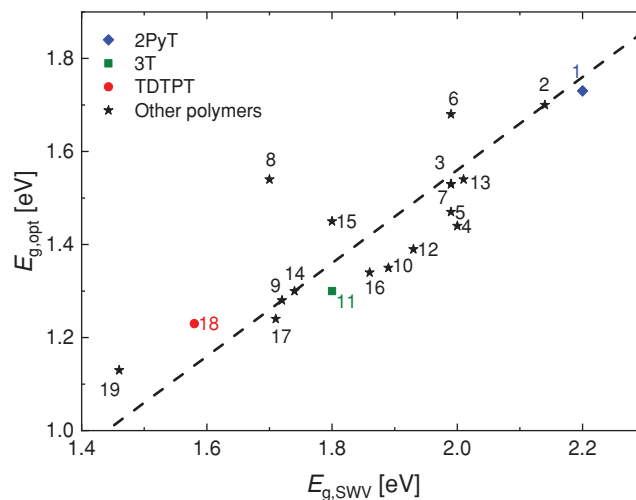


**Figure 4.** Correlation between the optical gap and the electrochemical gap. The dashed line is a fit to the data with fixed slope 1 and connects points for which the difference between both gaps is equal to 0.44 eV. Several polymers that have a smaller difference (6, 8, 15, 18, and 19) are discussed in the text. The optical and electrochemical gaps of 3 are equal to those of 7.

holds for two other polymers that have an electron-rich DTP unit, i.e., TDTP (18) and SDTPS (19), but for which the thienophene-2,5-diyl and selenophen-2-yl units that flank the DPP unit are more electron rich than the pyridine-2,6-diyl unit in 2PyDTP (8). For 2Py3T (6), the lower  $E_b = 0.31$  eV is a result of the combination of an electron-deficient 2Py-DPP-2Py segment as in 8 with an electron-rich 3T (terthiophene) segment. 3T is more electron rich than 1T and 2T units in 2PyT (1) and 2Py2T (2), but less than DTP in 2PyDTP (8). Finally, 5T (15) has the longest electron-rich segment, combined with DPP, in which case the centers of positive and negative charge densities of a CT-like absorption are more spatially separated.

In summary, the effective binding energy for the DPP polymers defined as  $E_b = E_{g,SWV} - E_{g,opt}$  amounts to about 0.44 eV for most DPP polymers, but can be significantly smaller when electronically distinct units are alternating along the chain.

## 2.2. Ultraviolet Photoelectron Spectroscopy

Whereas Equation (2) establishes a useful expression that may be used to predict  $V_{oc}$  from electrochemical experiments, it is of interest to investigate whether the relationship remains valid when using alternative methods for determining the HOMO energy. For that purpose, the HOMO energy was measured using UPS on thin polymer films on an ITO substrate. As an example, the high-energy and low-energy edges of the UPS spectra of 2PyT (1), 3T (11), and TDTP (18) are shown in Figure 5. The HOMO energy was determined from the kinetic energy difference,  $\Delta E$ , between the low-energy secondary-electron emission onset in the UPS spectrum and the high-energy edge, using the expression  $E_{HOMO,UPS} = \Delta E - E_{He-I}$ , where  $E_{He-I} = 21.22$  eV is the photon energy of the He-I radiation used. The cutoff energies used for determining the HOMO energies were obtained using a tangent method, as discussed in the Experimental Section. The experimental uncertainty is

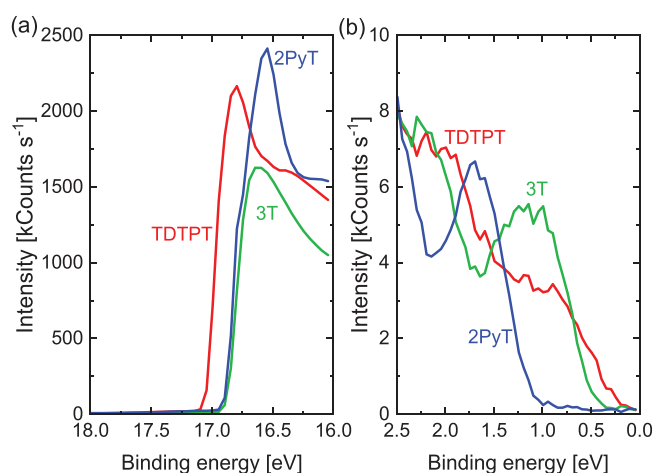


**Figure 5.** Ultraviolet photoelectron spectra for 2PyT (1), 3T (11), and TDTP (18): a) near the high-binding-energy edge, where the emission shows a peak due to secondary electrons and b) near the low-binding-energy edge. The HOMO energy,  $E_{HOMO,UPS}$ , is determined by drawing tangents through the inflection points in the spectra near both edges, as discussed in the Experimental Section.

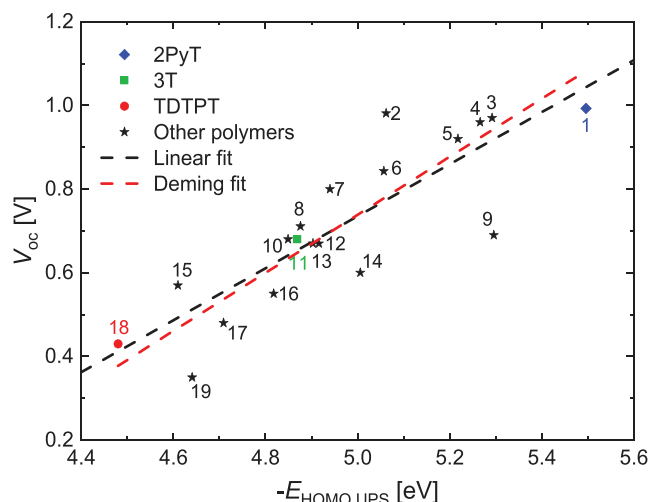


**Figure 6.** Correlation between the HOMO energies, measured using UPS, and the open-circuit voltage of optimized solar cells formed by blends with PC<sub>61</sub>BM or PC<sub>71</sub>BM. The black dashed line is the linear regression fit, given by Equation (3). The red dashed line represents a Deming regression with slope 0.69 and  $R^2 = 0.72$ .

somewhat larger than in the case of SWV, in most cases more close to  $\pm 0.10$  eV, as a result of the combined effects of the instrumental resolution ( $\pm 0.05$  eV) and the uncertainties in determining the leading and trailing edge binding energies. In some cases, substructures observed near the low-binding-energy edge give rise to a somewhat larger uncertainty. A complete overview of all spectra is included in the Supporting Information. The HOMO energies,  $E_{HOMO,UPS}$ , are listed in Table 1. Consistent with the results obtained from the electrochemical measurements, polymers incorporating pyridine-2,6-diyl or thiazoyl-2,5-diyl substituents are found to have the highest ionization energies (most negative HOMO energies).

Figure 6 shows the correlation between the measured HOMO energies and the  $V_{oc}$ . The best fit is given by the expression

$$qV_{oc} = -(0.62 \pm 0.09)E_{HOMO,UPS} - (2.3 \pm 0.5) \text{ [eV]} \quad (3)$$

For this fit,  $R^2 = 0.72$  is much smaller than  $R^2 = 0.94$  obtained for the correlation between  $V_{oc}$  and the oxidation potential from SWV (Figure 3). At least in part, this is due to the larger experimental uncertainty involved in the determination of the HOMO values from UPS, as discussed above. The largest deviations from the fit line are observed for the polymers 2Py2T (2), 2TzDTP (9), and SDTPS (19). However, for these three materials the onset at both spectral edges is clearly defined and the HOMO energy could be quite accurately determined. In this case, a Deming regression gives a slightly higher slope of 0.69, also with  $R^2 = 0.72$ .

Equation (3) also suggests a linear relation between  $V_{oc}$  and  $E_{HOMO}$  with slope less than unity. Yoshida has studied the correlation between the  $V_{oc}$  of PC<sub>61</sub>BM- and PC<sub>71</sub>BM-based solar cells based on blends with various polymers such as poly(3-hexylthiophene-2,5-diyl), poly(2,5-bis(3-tetradecylthiophen-2-yl)thieno[3,2-*b*]thiophene), and poly[2-methoxy-5-(3,7-dimethyloctyloxy)-1,4-phenylenevinylene].<sup>[52]</sup>  $V_{oc}$  was found to

be linearly correlated with the difference between the LUMO energy as determined using low-energy inverse photoelectron spectroscopy (LEIPS) and the HOMO energy as determined using UPS, in a manner as given by the expression

$$qV_{oc} = -(0.62 \pm 0.01)(E_{HOMO,UPS,D} - E_{HOMO,LEIPS,A}) [eV] \quad (4)$$

Making use of the LUMO energy of PC<sub>61</sub>BM that was found in ref. [52],  $-(3.84 \pm 0.04)$  eV, Equation (4) can be rewritten as

$$qV_{oc} = -0.62E_{HOMO,UPS,D} - 2.38 [eV] \quad (5)$$

which is virtually identical to fit in Equation (3). We note that the LUMO energy as obtained in ref. [52] for PC<sub>71</sub>BM,  $-(3.81 \pm 0.06)$  eV, is within the error margin equal to that of PC<sub>61</sub>BM. Hence, our results are consistent with the empirical finding by Yoshida that the  $V_{oc}$  varies linearly with the difference between the donor HOMO and the acceptor LUMO energies (determined by UPS and LEIPS), with a proportionality constant that is significantly smaller than unity.

### 2.3. Density Functional Theory

DFT calculations were performed on dimers of the repeat units of the DPP polymers. Ionization potential values were calculated by using the  $\Delta$ SCF method in which the geometry of the molecule is first optimized in the electronic ground state. This yields the ground state energy that serves as the reference value. Subsequently, an electron is removed from the system after which an open-shell DFT energy calculation is performed. The difference between the two energies yields the HOMO energy levels,  $E_{HOMO,\Delta SCF}$ ,<sup>[53]</sup> listed in Table 1. More details such as plots of the HOMO wave function are collected in the Supporting Information. **Figure 7** shows the relation between

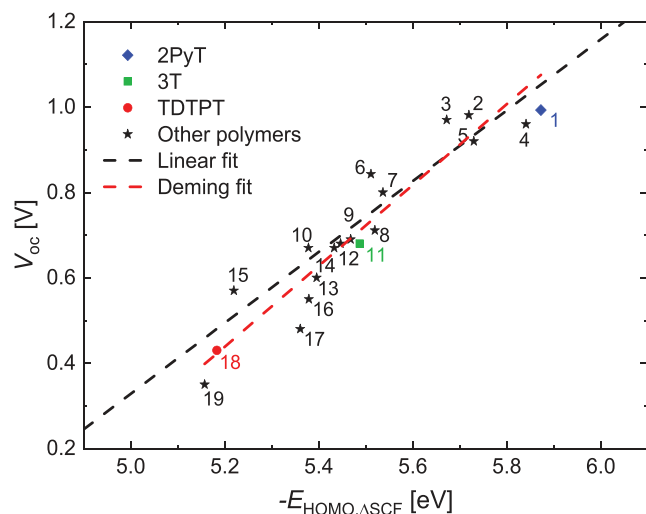


**Figure 7.** Correlation between the HOMO energies, from DFT calculations, and the open-circuit voltage of optimized solar cells formed by blends with PC<sub>61</sub>BM or PC<sub>71</sub>BM. The black dashed line is the linear regression fit, given by Equation (6). The red dashed line represents a Deming regression with slope 0.95 and  $R^2 = 0.89$ .

$E_{HOMO,\Delta SCF}$  and the  $V_{oc}$  of solar cells, made using blends of the polymer with PC<sub>61</sub>BM or PC<sub>71</sub>BM. As for SWV and UPS, there is a clear correlation between  $E_{HOMO,\Delta SCF}$  and  $V_{oc}$ . A least-squares fit gives

$$qV_{oc} = -(0.90 \pm 0.08)E_{HOMO,\Delta SCF} - (4.2 \pm 0.4) [eV] \quad (6)$$

with  $R^2 = 0.89$ . Compared to the relation between  $E_{ox,SWV}$  and  $V_{oc}$ , the spread on the data is larger for  $E_{HOMO,\Delta SCF}$ , but less than that for  $E_{HOMO,UPS}$  and  $V_{oc}$ . The slope in this case is close to unity. This is confirmed in the Deming regression, which gives a slope of 0.95 (Figure 7).

### 2.4. Correlation between the HOMO Energy from SWV, UPS, and DFT

**Figure 8** shows the correlation between the measured HOMO energies obtained from UPS and the oxidation potential measured using SWV, versus  $Fc/Fc^+$ . The best fit is given by the expression

$$E_{HOMO,UPS} = -(0.91 \pm 0.13)qE_{ox,SWV} - (4.59 \pm 0.06) [eV] \quad (7)$$

with  $R^2 = 0.74$ . Similar fits can be made to relate the DFT results to SWV and UPS data (Figure S2, Supporting Information)

$$E_{HOMO,\Delta SCF} = -(0.75 \pm 0.08)qE_{ox,SWV} - (5.18 \pm 0.04) [eV] \quad (8)$$

$$E_{HOMO,\Delta SCF} = (0.67 \pm 0.09)E_{HOMO,UPS} + (2.15 \pm 0.44) [eV] \quad (9)$$

with  $R^2 = 0.85$  and  $R^2 = 0.77$ , respectively.

The standard error found for the slope in Equation (7) suggests that the data can also be reasonably fitted with a slope of 1. In this case, Deming regression gives a slope of 1.07 (Figure 8). Hence, our results cannot be interpreted as

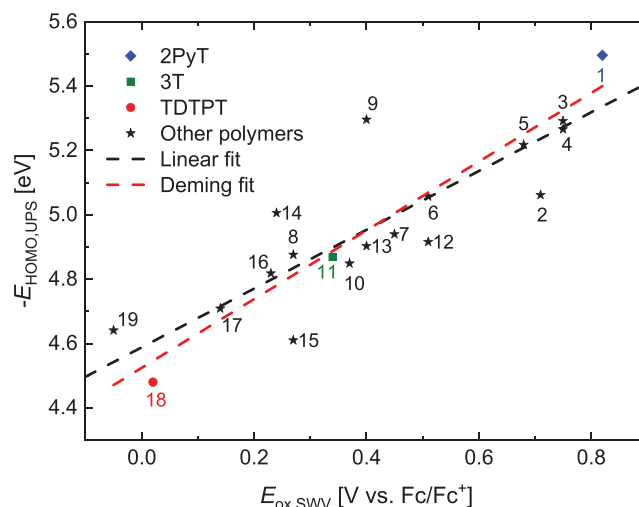


**Figure 8.** Correlation between the HOMO energies measured using UPS and SWV. The black dashed line is the linear regression fit given by Equation (7). The red dashed line represents a Deming regression with slope 1.07 and  $R^2 = 0.74$ .



evidence for a slope deviating from unity. A similar conclusion was recently reached by Wang et al. for ten different conjugated polymers where the slope was  $-(1.03 \pm 0.13)$  and the offset was  $-(4.54 \pm 0.08)$  eV.<sup>[40]</sup>

The spread in the data around the best-fit line in Figure 8 can be partially attributed to the experimental uncertainty of the data points: about  $\pm 0.05$  eV for  $E_{\text{HOMO,SWV}}$  and about  $\pm 0.10$  eV or in some cases slightly more for  $E_{\text{HOMO,UPS}}$ . We note that deviations larger than these error margins cannot be explained on the basis of an exceptionally large uncertainty in the analysis of the UPS spectra or SWV data. The largest deviation from the best fit is obtained for polymer 9 (2TzDTP) for which Figure 6 shows that  $E_{\text{HOMO,UPS}}$  is more negative than the expected value based on  $V_{\text{oc}}$ .

Equation (7) places  $E_{\text{Fc}/\text{Fc}^+}$  at  $-4.59$  eV versus the vacuum level. Using this value, we have determined the SWV HOMO energies ( $E_{\text{HOMO,SWV}}$ ) in Table 1. We can also use this value to determine the LUMO energy level of PC<sub>61</sub>BM using the redox potentials measured with SWV (Figure S3, Supporting Information). Using the experimental value of  $E_{\text{red,SWV}} = -0.98$  V versus Fc/Fc<sup>+</sup> and  $E_{\text{Fc}/\text{Fc}^+} = -4.59$  eV, we find a  $E_{\text{LUMO,SWV}} = -3.61$  eV for PC<sub>61</sub>BM, which is in fair agreement with value of  $-(3.84 \pm 0.04)$  eV found by Yoshida.<sup>[52]</sup>

Of course, UPS and SWV are not expected to yield in all cases the same value of the HOMO energy. Most importantly, the ionization energies probed are electrostatically screened to different extents, due to the different local environments in which the ionized molecules reside. In UPS, the signal originates predominantly from molecules at the surface, where the screening due to the polarizability of the environment is weaker than that in the bulk.<sup>[30]</sup> The signal as probed by voltammetry of molecules in solution is influenced by the screening by the metal electrode and by the electrolyte solution.<sup>[36]</sup> In the case of voltammetry on thin films, it is not well known to what extent the ionization process takes place at the outer film surface, in contact with the electrolyte, or in the bulk of the thin film. In any case, also the presence of the electrolyte and the metal electrode will affect the redox potential. Additional complications include 1) the effect of the vacuum surface or the interface with the electrolyte on the energetic disorder, 2) the different roles of molecular relaxation during the excitation, and 3) the different roles of possible surface or bulk contaminants. These effects may also depend on the specific material properties.

## 2.5. Correlation between HOMO Energies and $V_{\text{oc}}$

The oxidation potential determined using SWV is a good predictor for the  $V_{\text{oc}}$  of the DPP polymers in combination with PCBM as an acceptor via Equation (2). In a recent study, Fahlman and coworkers argued that CV estimates of the ionization potential are too imprecise compared to the UPS data for determining energy levels at donor–acceptor heterojunctions. Our study clearly shows that this is not the case. Moreover, the conclusion of Fahlman and coworkers is not in accordance with our own analysis of their data, which shows the same (moderate) correlation of  $V_{\text{oc}}$  with the either  $E_{\text{ox,CV}}$  ( $R^2 = 0.64$ ) or  $E_{\text{HOMO,UPS}}$  ( $R^2 = 0.62$ ) (Table S1 and Figure S4, Supporting Information).

Remarkably, the slope of the fitted data is 0.75 in Equation (2) with a standard error of  $\pm 0.04$ . For UPS, the slope of  $0.62 \pm 0.09$  is also less than unity (Equation (3)), and consistent with the value reported by Yoshida.<sup>[52]</sup> Hence, both SWV and UPS experiments reveal that for these DPP polymers, and their solar cells with PCBM, the linear correlation between  $V_{\text{oc}}$  and ( $E_{\text{HOMO,D}} - E_{\text{LUMO,A}}$ ) has a slope less than unity. In contrast, we note that Scharber et al., in a study on 26 different bulk heterojunction blends, found a correlation with a slope equal to 1 between  $V_{\text{oc}}$  and the redox potential difference.<sup>[21]</sup> A linear correlation between  $V_{\text{oc}}$  and the HOMO and LUMO energies with slope 1 has also been seen in various other studies,<sup>[6,54]</sup> usually for a smaller set of materials, but deviations with slope  $< 1$  have also been reported.<sup>[52,55]</sup>

At present, it is not possible to resolve the discrepancies between these various studies. Nevertheless, it is of interest to consider possible explanations for our finding of a slope  $< 1$ . One effect to be considered is the dependence of the generation rate  $G$  on the HOMO level. DPP polymers with higher HOMO energy tend to have lower optical band gap and can therefore generate more charges. For solar cells of the polymers in Table 1, 2PyT ( $E_{\text{g}} = 1.73$  eV) gave the lowest short-circuit current density ( $J_{\text{sc}}$ ) ( $7.00$  mA cm<sup>-2</sup>),<sup>[56]</sup> while TDPT ( $E_{\text{g}} = 1.23$  eV) gave the highest  $J_{\text{sc}}$  ( $20.5$  mA cm<sup>-2</sup>),<sup>[57]</sup> i.e., a factor of  $\approx 3$ . Assuming that  $G$  is proportional to  $J_{\text{sc}}$ , one would expect a difference of  $(kT/q)\ln(3) = 28$  mV via Equation (1), which is an order of magnitude too low to explain a change in slope from 1 to 0.75.

One option to explain the reduced slope is that the HOMO of the donor and LUMO of the acceptor interact, resulting in a rearrangement of the HOMO and LUMO energy levels of the donor and acceptor molecules involved in the formation of the CT state,  $E_{\text{HOMO}}^{\text{CT}}$  and  $E_{\text{LUMO}}^{\text{CT}}$ , compared to those of the constituents,  $E_{\text{HOMO}}^{\text{D}}$  and  $E_{\text{LUMO}}^{\text{A}}$ . We find that such effect can explain the reduced slope quantitatively using first-order perturbation theory when assuming a large interaction energy  $H_{\text{DA}}$  of 0.4–0.5 eV (see the Supporting Information). Theoretical studies show that such large transfer integrals exist for cofacially arranged charge-transfer donor–acceptor cocrystals at short distances.<sup>[58,59]</sup> It is, however, far from clear whether such large transfer integrals are possible in polymer–fullerene blends, where both large ( $\approx 0.3$  eV)<sup>[22]</sup> and very small ( $\approx 0.01$  eV)<sup>[60]</sup> transfer integrals have been reported, for seemingly similar systems. We note that transfer integrals between adjacent molecules in organic materials larger than  $\approx 0.01$  eV would give rise to delocalization of electron and hole states, which is not commonly observed. Other theoretical studies have shown that the charge-transfer state energy can vary by 0.2–0.6 eV, depending on the relative orientation of donor and acceptor molecules.<sup>[61]</sup> Via Equation (1), this would result in a change in  $V_{\text{oc}}$  of 0.2–0.6 V.

Experimental studies also do not provide a completely consistent insight. In a recent experimental study on the energy alignment at pentacene/C<sub>60</sub> interfaces, it was shown that the HOMO–LUMO gap at the interface varies from 1.50 eV for a face-on orientation to 0.75 eV for an edge-on arrangement of the molecules.<sup>[62]</sup> This is consistent with earlier work in which it was shown that interface energies of sexithiophene depend on the orientation of the molecules with respect to the interface.<sup>[63]</sup> On the other hand, the HOMO–LUMO gap at the interface

between diindenoperylene and C<sub>60</sub> was found to be identical to that based on the HOMO and LUMO energies of the pristine materials.<sup>[54]</sup> In their review, Koch and coworkers conclude that predicting the interface dipole is difficult,<sup>[23]</sup> but from a more recent study on blends of five commonly used conjugated polymers with PCBM one can infer that the vacuum level shift scales with  $E_{\text{HOMO,D}}$ .<sup>[7]</sup> The vacuum level shift ( $\Delta$ ) and  $E_{\text{HOMO,D}}$  from ref. [7] are collected in Table S2 and Figure S6 in the Supporting Information. A fit gives  $\Delta = (0.33 \pm 0.09)E_{\text{HOMO,D}} + (1.76 \pm 0.43)$  [eV]. Although the number of data points (5) is limited and the correlation ( $R^2 = 0.88$ ) is not perfect, the vacuum level shift indeed decreases with more negative  $E_{\text{HOMO,D}}$ . Because  $\Delta$  increases the offset between  $E_{\text{HOMO,D}}$  and  $E_{\text{LUMO,A}}$  at the donor–acceptor interface, it increases the  $V_{\text{oc}}$  for donors with a low oxidation potential. In fact, when the slope of 0.33 is added to the slope of 0.75 found in our work, a total slope of 1.08 emerges, which is (probably somewhat fortuitously) identical to the slope of 1.08 recently found by Vandewal and coworkers between  $qV_{\text{oc}}$  and  $E_{\text{CT}}$ .<sup>[10]</sup>

In summary, both theoretical and experimental studies suggest that different molecular orientations can give rise to differences in  $E_{\text{CT}}$  at the donor–acceptor interface, amounting up to several tenths of an electron volt. While such deviations can explain the difference between a slope of 0.75 and a slope of 1, over the  $\approx 1$  eV range of HOMO energies (Figure 2), they do not give a rationale for the result that  $V_{\text{oc}}$  (and hence  $E_{\text{CT}}$ ) would change in gradual fashion with the HOMO energy, which is suggested by the small scatter ( $<0.1$  eV) in the experimental data with respect to the fit (Figure 2). Possibly, the formation of an interface dipole at the DPP polymer–PCBM interface,<sup>[23]</sup> which one can expect to be dependent on the HOMO level of the donor, explains the slope of less than 1 found in a plot of  $V_{\text{oc}}$  versus  $E_{\text{ox,SWV}}$  (Figure 3).

### 3. Conclusion

In summary, the HOMO energy levels of 19 different DPP polymers have been investigated using SWV, UPS, and DFT and have been compared to the  $V_{\text{oc}}$  of bulk heterojunction solar cells of these polymers as donor in combination with PCBM as acceptor. The polymers, solar cells, and electrochemical and photoelectron spectroscopy experiments all have been prepared, performed, and analyzed with identical procedures. The results reveal that the SWV redox potential ( $E_{\text{ox,SWV}}$ ) is the most accurate predictor of the open-circuit voltage ( $V_{\text{oc}}$ ). Remarkably, the slope of the linear relation between  $V_{\text{oc}}$  and  $E_{\text{ox,SWV}}$  is  $0.75 \pm 0.04$ , i.e., significantly less than 1.

The oxidation potentials determined by SWV versus Fc/Fc<sup>+</sup> and the HOMO energies determined by UPS are linearly correlated with a slope of  $0.91 \pm 0.13$  eV V<sup>-1</sup>, which statistically does not differ from unity. The intercept places the energy of the ferrocene/ferrocenium redox couple ( $E_{\text{Fc/Fc}^+}$ ) at  $-4.59$  eV versus vacuum. The linear relationship between  $V_{\text{oc}}$  and  $E_{\text{HOMO,UPS}}$  has a slope of  $0.62 \pm 0.09$  V eV<sup>-1</sup>, in excellent agreement with earlier work.<sup>[52]</sup>

Possible reasons for a slope of less than 1 for the relation between the HOMO energy measured on the pure donor material and  $V_{\text{oc}}$  in the blend were discussed. Possibly, a dipole at

the donor–acceptor interface, whose magnitude depends on the HOMO level of the donor,<sup>[7]</sup> can explain the result. A full consistent insight, however, requires further examination in future work.

For the DPP polymers, the electrochemical band gap ( $E_{\text{g,SWV}} \equiv q(E_{\text{ox,SWV}} - E_{\text{red,SWV}})$ ) is linearly and with unit slope correlated to the optical band gap ( $E_{\text{g,opt}}$ ). The average difference is  $0.44 \pm 0.10$  eV, but actual values vary from 0.16 to 0.56 eV. Low values are found for DPP polymers in which there is a more pronounced difference between the electron-deficient and electron-rich moieties that could result in a more localized character of the electron and hole wave functions in the excited state.

In this study, we have demonstrated that the oxidation potential determined with square-wave voltammetry on thin polymer films, as first employed by Inganäs, Andersson, and coworkers,<sup>[32]</sup> is a very good and accessible experimental method to forecast the open-circuit voltage of organic bulk heterojunction solar cells. Results from ultraviolet photoelectron spectroscopy provide a less accurate prediction.

### 4. Experimental Section

**Cyclic and Square-Wave Voltammetry:** Cyclic voltammetry and square-wave voltammetry measurements were performed inside a nitrogen-filled glove box using an Autolab PGSTAT30 (Ecochemie, The Netherlands) potentiostat in a three-electrode configuration. A polymer-coated platinum wire, silver wire, and silver/silver chloride (Ag/AgCl) electrode served as working electrode, counter electrode, and quasi-reference electrode, respectively. A 0.1 M solution of tetrabutylammonium hexafluorophosphate (TBAPF<sub>6</sub>) in dry acetonitrile served as electrolyte. All potentials were reported versus the ferrocene/ferrocenium redox couple (Fc/Fc<sup>+</sup>). The used ionization energy of ferrocene was 4.59 eV, as derived from a comparison with the UPS results in this study. Before each measurement, the platinum wire working electrode was cleaned in a roaring blue flame. The polymer films were applied on the platinum wire by dipping the wire for several seconds into a 2 mg mL<sup>-1</sup> solution of the polymer in chloroform, which has been stirred at 60 °C for at least 2 h. For cyclic voltammetry, the potential was stepwise ramped with a step potential of 2.4 mV and an average scan speed of 0.1 or 0.126 V s<sup>-1</sup>. No significant difference between the results obtained for these two scan speeds was found. The square-wave voltammetry experiments were performed with a step potential of 5 mV and an average scan speed of 0.126 V s<sup>-1</sup>. On each step, a square-wave modulation was used with an amplitude of 20 mV, a period equal to the step length (0.04 s), and a phase such that in the first (second) half of the step a potential overshoot (undershoot) was obtained. In order to exclude effects of repetitive oxidation and reduction on the voltammogram, all data presented were taken from the first scan. The onsets were determined using a tangent method, where the onset was placed at the intercept of the linearly extrapolated tangent with the baseline. In the square-wave voltammograms shown in the Supporting Information, the position of the onset is indicated.

**Ultraviolet Photoelectron Spectroscopy:** The UPS measurements were performed in a multichamber EscaLab II system with a base pressure of the analyzer chamber in the lower 10<sup>-8</sup> Pa range. The UPS spectra were recorded using He-I radiation (photon energy  $E_{\text{He-I}} = 21.22$  eV) generated in a differentially pumped, windowless discharge lamp. As the investigated polymers were sensitive to UV radiation, the UV exposure during UPS was kept to a minimum at the cost of a higher noise level. The measurements were performed with an applied bias of  $-6$  V.

To prepare the samples for UPS measurements, a 2 mg mL<sup>-1</sup> solution of the polymer in anhydrous chloroform was stirred at 60 °C for at least 1 h, in a nitrogen-filled glove box. ITO substrates were cleaned by rinsing with acetone and both mechanical rubbing and rinsing with

isopropanol, followed by a 30 min UV–ozone treatment. The solution was subsequently spin coated at 2000 rpm for 60 s inside the glove box on cleaned ITO substrates. Samples were transferred through air to the UPS setup, except for 3T (11), TPYT (16), SPyS (17), and SDTPS (19), which were transported in a nitrogen-filled transfer tube to prevent oxidation of the thin layers of these low–band gap materials.

The HOMO energy was determined from the kinetic energy difference,  $\Delta E$ , between the low-energy secondary-electron emission onset of the UPS spectrum and the high-energy edge using the expression  $E_{\text{HOMO,UPS}} = \Delta E - E_{\text{HE-I}}$ , where  $E_{\text{HE-I}} = 21.22$  eV. The edge energies were obtained by linearly extrapolating tangents through the point of inflection in the low-energy and high-energy slopes to the background level. The positions of the onsets are indicated in the spectra in the Supporting Information. The binding energy was defined with respect to the Fermi level:  $E_{\text{bind}} = E_f - E_{\text{kin}}$ . The Fermi level was located at a kinetic energy of 27.49 eV.

**Density Functional Theory Calculations:** Ionization potential values were calculated by using the  $\Delta$ SCF method as described in the text. All calculations were performed employing the B3LYP functional with a 6–31g\* basis set. The NWCHEM software package was used for the calculations.<sup>[64]</sup>

## Supporting Information

Supporting Information is available from the Wiley Online Library or from the author.

## Acknowledgements

The authors thank Prof. Weiwei Li, Dr. Koen Hendriks, Gaël Heintges, Dr. Ruurd Heuvel, and Dr. Mathieu Turbiez for providing the polymers used in this research and Dr. Stefan Meskers for fruitful discussions. The work was performed in the framework of the Triple Solar (ERC Advanced Grant No. 339031) projects, the Horizon-2020 EU project MOSTOPHOS (Project No. 646259), and received funding from the Ministry of Education, Culture and Science of Netherlands (Gravity program 024.001.035).

## Conflict of Interest

The authors declare no conflict of interest.

## Keywords

density functional theory, open-circuit voltage, organic photovoltaics, square-wave voltammetry, ultraviolet photoelectron spectroscopy

Received: November 27, 2018

Revised: December 23, 2018

Published online: January 28, 2019

- [1] K. Vandewal, *Annu. Rev. Phys. Chem.* **2016**, *67*, 113.
- [2] L. J. A. Koster, V. D. Mihailetschi, R. Ramaker, P. W. M. Blom, *Appl. Phys. Lett.* **2005**, *86*, 123509.
- [3] W. Tress, K. Leo, M. Riede, *Phys. Rev. B* **2012**, *85*, 155201.
- [4] Z. Teng, B. Erik, L. Joachim, *Appl. Phys. Express* **2015**, *8*, 024301.
- [5] K. Vandewal, K. Tvingstedt, A. Gadisa, O. Inganäs, J. V. Manca, *Phys. Rev. B* **2010**, *81*, 125204.

- [6] J. Widmer, M. Tietze, K. Leo, M. Riede, *Adv. Funct. Mater.* **2013**, *23*, 5814.
- [7] Q.-D. Yang, H.-W. Li, Y. Cheng, Z. Guan, T. Liu, T.-W. Ng, C.-S. Lee, S.-W. Tsang, *ACS Appl. Mater. Interfaces* **2016**, *8*, 7283.
- [8] D. Veldman, S. C. J. Meskers, R. A. J. Janssen, *Adv. Funct. Mater.* **2009**, *19*, 1939.
- [9] W. Li, K. H. Hendriks, A. Furlan, M. M. Wienk, R. A. J. Janssen, *J. Am. Chem. Soc.* **2015**, *137*, 2231.
- [10] J. Benduhn, K. Tvingstedt, F. Piersimoni, S. Ullbrich, Y. Fan, M. Tropiano, K. A. McGarry, O. Zeika, M. K. Riede, C. J. Douglas, S. Barlow, S. R. Marder, D. Neher, D. Spoltore, K. Vandewal, *Nat. Energy* **2017**, *2*, 17053.
- [11] R. Marcus, *J. Phys. Chem.* **1989**, *93*, 3078.
- [12] I. R. Gould, D. Noukalcis, L. Gomez-Jahn, R. H. Young, J. L. Goodman, S. Farid, *Chem. Phys.* **1993**, *176*, 439.
- [13] Z. Guan, H.-W. Li, Y. Cheng, Q. Yang, M.-F. Lo, T.-W. Ng, S.-W. Tsang, C.-S. Lee, *J. Phys. Chem. C* **2016**, *120*, 14059.
- [14] A. Weller, *Z. Phys. Chem.* **1982**, *133*, 93.
- [15] J. B. Torrance, J. E. Vazquez, J. J. Mayerle, V. Y. Lee, *Phys. Rev. Lett.* **1981**, *46*, 253.
- [16] D. V. Konarev, R. N. Lyubovskaya, N. V. Drichko, V. N. Semkin, A. Graja, *Chem. Phys. Lett.* **1999**, *314*, 570.
- [17] D. V. Konarev, R. N. Lyubovskaya, N. V. Drichko, E. I. Yudanov, Y. M. Shul'ga, A. L. Litvinov, V. N. Semkin, B. P. Tarasov, *J. Mater. Chem.* **2000**, *10*, 803.
- [18] P. Panda, D. Veldman, J. Sweelssen, J. J. A. M. Bastiaansen, B. M. W. Langeveld-Voss, S. C. J. Meskers, *J. Phys. Chem. B* **2007**, *111*, 5076.
- [19] C. J. Brabec, A. Cravino, D. Meissner, N. S. Sariciftci, T. Fromherz, M. T. Rispen, L. Sanchez, J. C. Hummelen, *Adv. Funct. Mater.* **2001**, *11*, 374.
- [20] A. Gadisa, M. Svensson, M. R. Andersson, O. Inganäs, *Appl. Phys. Lett.* **2004**, *84*, 1609.
- [21] M. C. Scharber, D. Mühlbacher, M. Koppe, P. Denk, C. Waldauf, A. J. Heeger, C. J. Brabec, *Adv. Mater.* **2006**, *18*, 789.
- [22] S. M. Falke, C. A. Rozzi, D. Brida, M. Maiuri, M. Amato, E. Sommer, A. De Sio, A. Rubio, G. Cerullo, E. Molinari, C. Lienau, *Science* **2014**, *344*, 1001.
- [23] A. Opitz, J. Frisch, R. Schlesinger, A. Wilke, N. Koch, *J. Electron Spectrosc. Relat. Phenom.* **2013**, *190*, 12.
- [24] K. Seki, *Mol. Cryst. Liq. Cryst.* **1989**, *171*, 255.
- [25] K. H. Frank, P. Yannoulis, R. Dudde, E. E. Koch, *J. Chem. Phys.* **1988**, *89*, 7569.
- [26] H. Yoshida, *J. Electron Spectrosc. Relat. Phenom.* **2015**, *204*, 116.
- [27] H. Kirihaata, M. Uda, *Rev. Sci. Instrum.* **1981**, *52*, 68.
- [28] H. Ishii, H. Kinjo, T. Sato, S. Machida, Y. Nakayama, in *Electronic Processes in Organic Electronics* (Eds: H. Ishii, K. Kudo, T. Nakayama, N. Ueno), Springer, Tokyo, Japan **2015**, Ch. 8, pp. 131–155.
- [29] R. J. Davis, M. T. Lloyd, S. R. Ferreira, M. J. Bruzek, S. E. Watkins, L. Lindell, P. Sehati, M. Fahlman, J. E. Anthony, J. W. P. Hsu, *J. Mater. Chem.* **2011**, *21*, 1721.
- [30] W. R. Salaneck, *Phys. Rev. Lett.* **1978**, *40*, 60.
- [31] J. G. Osteryoung, R. A. Osteryoung, *Anal. Chem.* **1985**, *57*, 101A.
- [32] S. Hellström, F. Zhang, O. Inganäs, M. R. Andersson, *Dalton Trans.* **2009**, 10032.
- [33] L. Ramaley, M. S. Krause, *Anal. Chem.* **1969**, *41*, 1362.
- [34] G. Gritzner, J. Kuta, *Pure Appl. Chem.* **1984**, *56*, 461.
- [35] C. M. Cardona, W. Li, A. E. Kaifer, D. Stockdale, G. C. Bazan, *Adv. Mater.* **2011**, *23*, 2367.
- [36] B. W. D'Andrade, S. Datta, S. R. Forrest, P. Djurovich, E. Polikarpov, M. E. Thompson, *Org. Electron.* **2005**, *6*, 11.
- [37] P. I. Djurovich, E. I. Mayo, S. R. Forrest, M. E. Thompson, *Org. Electron.* **2009**, *10*, 515.
- [38] J. Sworakowski, J. Lipiński, K. Janus, *Org. Electron.* **2016**, *33*, 300.
- [39] J. Sworakowski, K. Janus, *Org. Electron.* **2017**, *48*, 46.

- [40] C. Wang, L. Ouyang, X. Xu, S. Braun, X. Liu, M. Fahlman, *Sol. RRL* **2018**, 2, 1800122.
- [41] W. Li, K. H. Hendriks, M. M. Wienk, R. A. J. Janssen, *Acc. Chem. Res.* **2016**, 49, 78.
- [42] H. Choi, S.-J. Ko, T. Kim, P.-O. Morin, B. Walker, B. H. Lee, M. Leclerc, J. Y. Kim, A. J. Heeger, *Adv. Mater.* **2015**, 27, 3318.
- [43] Y. Liu, G. Li, Z. Zhang, L. Wu, J. Chen, X. Xu, X. Chen, W. Ma, Z. Bo, *J. Mater. Chem. A* **2016**, 4, 13265.
- [44] M. Li, D. Di Carlo Rasi, F. J. M. Colberts, J. Wang, G. H. L. Heintges, B. Lin, W. Li, W. Ma, M. M. Wienk, R. A. J. Janssen, *Adv. Energy Mater.* **2018**, 8, 1800550.
- [45] K. H. Hendriks, W. Li, G. H. L. Heintges, G. W. P. van Pruissen, M. M. Wienk, R. A. J. Janssen, *J. Am. Chem. Soc.* **2014**, 136, 11128.
- [46] S. D. D. V. Rughooputh, M. Nowak, S. Hotta, A. J. Heeger, F. Wudl, *Synth. Met.* **1987**, 21, 41.
- [47] W. E. Deming, *Statistical Adjustment of Data*. Wiley, New York **1943**.
- [48] J.-W. van der Horst, P. A. Bobbert, M. A. J. Michels, H. Bässler, *J. Chem. Phys.* **2001**, 114, 6950.
- [49] I. G. Hill, A. Kahn, Z. G. Soos, R. A. Pascal, *Chem. Phys. Lett.* **2000**, 327, 181.
- [50] M. Knupfer, *Appl. Phys. A* **2003**, 77, 623.
- [51] H. Yoshida, K. Yoshizaki, *Org. Electron.* **2015**, 20, 24.
- [52] H. Yoshida, *J. Phys. Chem. C* **2014**, 118, 24377.
- [53] R. O. Jones, O. Gunnarsson, *Rev. Mod. Phys.* **1989**, 61, 689.
- [54] A. Wilke, J. Endres, U. Hörmann, J. Niederhausen, R. Schlesinger, J. Frisch, P. Amsalem, J. Wagner, M. Gruber, A. Opitz, A. Vollmer, W. Brütting, A. Kahn, N. Koch, *Appl. Phys. Lett.* **2012**, 101, 233301.
- [55] B. P. Rand, D. P. Burk, D. R. Forrest, *Phys. Rev. B* **2007**, 75, 115327.
- [56] K. H. Hendriks, A. S. G. Wijkema, J. J. van Franeker, M. M. Wienk, R. A. J. Janssen, *J. Am. Chem. Soc.* **2016**, 138, 10026.
- [57] K. H. Hendriks, W. Li, M. M. Wienk, R. A. J. Janssen, *J. Am. Chem. Soc.* **2014**, 136, 12130.
- [58] L. Zhu, E.-G. Kim, Y. Yi, J.-L. Brédas, *Chem. Mater.* **2011**, 23, 5149.
- [59] R. Kumar Behera, N. R. Goud, A. J. Matzger, J.-L. Brédas, V. Coropceanu, *J. Phys. Chem. C* **2017**, 121, 23633.
- [60] T. Liu, A. Troisi, *J. Phys. Chem. C* **2011**, 115, 2406.
- [61] E. B. Isaacs, S. Sharifzadeh, B. Ma, J. B. Neaton, *J. Phys. Chem. Lett.* **2011**, 2, 2531.
- [62] T. Nishi, M. Kanno, M. Kuribayashi, Y. Nishida, S. Hattori, H. Kobayashi, F. von Wrochem, V. Rodin, G. Nelles, S. Tomiya, *Appl. Phys. Lett.* **2018**, 113, 163302.
- [63] S. Duhm, G. Heimel, I. Salzmann, H. Glowatzki, R. L. Johnson, A. Vollmer, J. P. Rabe, N. Koch, *Nat. Mater.* **2008**, 7, 326.
- [64] M. Valiev, E. J. Bylaska, N. Govind, K. Kowalski, T. P. Straatsma, H. J. J. Van Dam, D. Wang, J. Nieplocha, E. Apra, T. L. Windus, W. A. de Jong, *Comput. Phys. Commun.* **2010**, 181, 1477.